Document NWPSAF-KN-VS-016

Version 1.0

31-08-2016

ASCAT-6.25 validation on coastal jets - 2

Isabel Monteiro[1] , Jur Vogelzang[2] and Ad Stoffelen[2]

- ***IPMA, Lisbon, Portugal***
- ***KNMI, De Bilt, The Netherlands***

ASCAT-6.25 validation on coastal jets - 2

Isabel Monteiro (IPMA),
Jur Vogelzang and Ad Stoffelen (KNMI)

This documentation was developed within the context of the EUMETSAT Satellite Application Facility on Numerical Weather Prediction (NWP SAF), under the Cooperation Agreement dated 29 June 2011, between EUMETSAT and the Met Office, UK, by one or more partners within the NWP SAF. The partners in the NWP SAF are the Met Office, ECMWF, KNMI and Météo France.

Change record			
Version	Date	Author / changed by	Remarks
0.1	12-07-2016	J. Vogelzang	1st draft
0.2	15-07-2016	I. Monteiro	revision
0.3	30-08-2016	A. Stoffelen	revision
1.0	05-09-2016	J. Vogelzang	1st version

Introduction

In the period October 19-21, 2015, Isabel Monteiro from the Instituto Português do Mar e da Atmosfera (IPMA) made a first visit to the Royal Netherlands Meteorological Institute (KNMI) to discuss validation of the ASCAT-6.25 wind product in the framework of a study on coastal jets off the Iberian coast using model forecasts and buoy measurements. IPMA was beta user of the experimental ASCAT-6.25 product that became operational mid 2016 in version 2.4 of the ASCAT Wind Data Processor (AWDP) [*Verhoef et al.*, 2016]. The main aim of that mission was to exchange experiences with this new wind product in order to improve user guidance.

User guidance is important for ASCAT-6.25, since the Ocean and Sea Ice Satellite Application Facility (OSI SAF) decided not to issue a near real time ASCAT-6.25 wind product. One reason for this is that the ASCAT-6.25 wind product demands at least four times as much computer capacity as the ASCAT-coastal product. Another reason is that the ASCAT-6.25 wind product is primarily intended for studies of mesoscale features like von Kármán vortices in the lee of islands, convective processes, and coastal jets. Its user community is therefore expected to be smaller than that of the other ASCAT products, and interest will be restricted to specific areas.

The October 2015 VS mission led to a number of recommendations for further study [*Monteiro et al.*, 2015]. One of the recommendations was to process ASCAT-6.25 data for all summer months (June, July, and August) for the period 2010 - 2014 in order to have more buoy comparisons. Another recommendation was to reprocess ASCAT-6.25 with an aggregation radius of 15 km for the same period. The resulting wind product has the same characteristics the ASCAT-coastal product, but on a 6.25 km grid. This enables better comparison between the ASCAT-6.25 and ASCAT-coastal products, because collocations will have the same distance to the buoys for both products. In principle, the more detailed ASCAT-6.25 product could also be beneficial for nowcasting of cyclones . However, cyclone centers in ASCAT-6.25 are more prone to noise, QC rejections, and subsequent ambiguity removal errors because of the poorer radar statistics. It was therefore concluded that the ASCAT-coastal product is now more suited for such applications, but that this may change when QC, spatial processing, and ambiguity removal in AWDP is improved in the future.

During 2016 the study was extended with spatial statistical analysis. Also the question emerged how the buoy winds should be transformed in order to achieve the best comparability with scatterometer winds. It became clear that a second visit was necessary in order to discuss progress and exchange experiences.

This visit took place July 4-6, 2016. This document reports the progress made since the first visit and the results of the VS mission.

Study area

The study area is the Iberian west coast with special emphasis on the main capes: Cape Finisterra in the northwest, Cape Roca near Lisbon, and Cape São Vicente in the southwest (see figure 1). Under specific meteorological conditions in summertime a coastal jet develops offshore the Iberian peninsula with wind maxima linked to the main capes mentioned above.

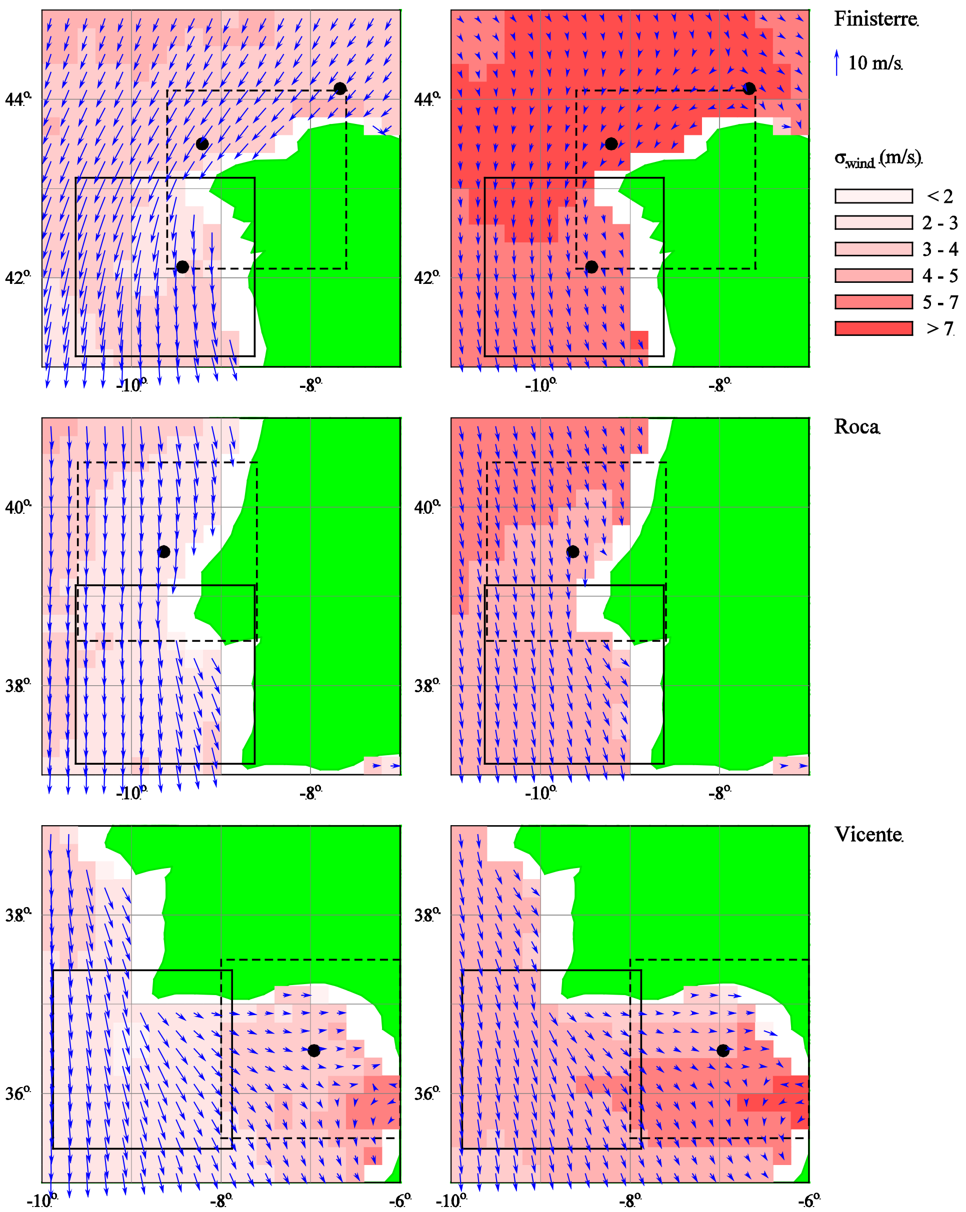

Figure 1 Average wind field during the whole study period under costal jet (CJ) conditions (left hand panels) and non coastal jet conditions (right hand panels) for the three study areas, where class CJ amounts to 15% of the ASCAT overpasses at Finisterre and Roca, and about 25% at Vicente.

This study spans the summer months (June, July, and August) in the years 2010 to 2014. Figure 1 shows the average wind field during this period averaged on a 0.2° by 0.2° grid for coastal jet conditions (left hand panels) and non coastal jet conditions (right hand panels) for each of the three areas of special interest (Finisterre, Roca, and Vicente, from north to south). Average wind vectors are in blue, with their length proportional to the wind speed (see the legend for the reference wind speed of 10 m/s). The background colors indicate the variation in the wind. The solid squares measure 2° by 2° and are centered around the position where the maximum wind speed is found under coastal jet (CJ) conditions. These areas are used for the spatial statistics analysis reported below. The black dots indicate the buoy positions.

An event is classified as a costal jet (CJ) if the wind speed at the centre of the jet area exceeds a threshold value (see table 1 for the definition of the areas and the threshold wind speed), and if the wind direction exceeds 292.5° true North but is less than 67.5 true North. The location of the jet maximum and the threshold wind speed were determined from 10 years of QuikSCAT data.

Any other event is labeled as a non coastal jet event (nonCJ), except for Finisterre where a third class is defined: that of the wind reversals (WR). This class is characterized by passage of a front. Frontal passages at Roca and Vicente are rare: for 10 years of QuikSCAT data only 30 events were found. Therefore wind reversals are not considered as a separate class for Roca and Vicente.

Area	Centre latitude	Centre longitude	Threshold wind speed (m/s)
Finisterre	42.12	-9.625	10.5
Roca	38.125	-9.625	10.8
Vicente	36.38	-8.875	10.1

Table 1 Coastal jet classification criteria.

At Finisterre and Roca 15% of the ASCAT overpasses were classified as coastal jets; at Vicente 22%

Data

The data used in this study are:

- Ordinary ASCAT-6.25 data (7.5 km aggregation radius) for the summer months (June, July and August) in the period 2010 - 2014;
- ASCAT-6.25 data with 15.0 km aggregation radius for the same period;
- Buoy data from five offshore buoys for the period 2010 - 2014. Figure 1 shows that the buoys are far enough offshore to be within the measurement range of ASCAT.
- ERA-interim and ECMWF IFS forecasts.

The ASCAT data were processed according to the recommendations from the 2015 VS mission [*Monteiro et al.*, 2015]. The ordinary ASCAT-6.25 product will further be referred to as ASCAT-6.25; the product with 15 km aggregation radius as (oversampled) ASCAT-coastal. The scatterometer data were divided in two categories: coastal jets (CJ) and - the remaining data - non coastal jets (non-CJ). Only for Finisterre a third category was introduced: wind reversals (WR), characterized by the passing of fronts. For the other regions such events were too rare to be of statistical importance.

Results

General

Visual inspection of the ASCAT-coastal and ASCAT-6.25 wind fields during coastal jet conditions already revealed that the wind maxima are sharper and deeper in ASCAT-6.25 than in ASCAT-coastal.

Figure 1 also contains some general information. Under coastal jet conditions the wind is generally stronger than under non coastal jet conditions, and the variation in the wind is lower. Note that the wind tends to bend around the capes and towards the land. This is likely to be caused by a sea breeze effect: all data are recorded during summer when the land heats quickly, causing lower surface pressure above land.

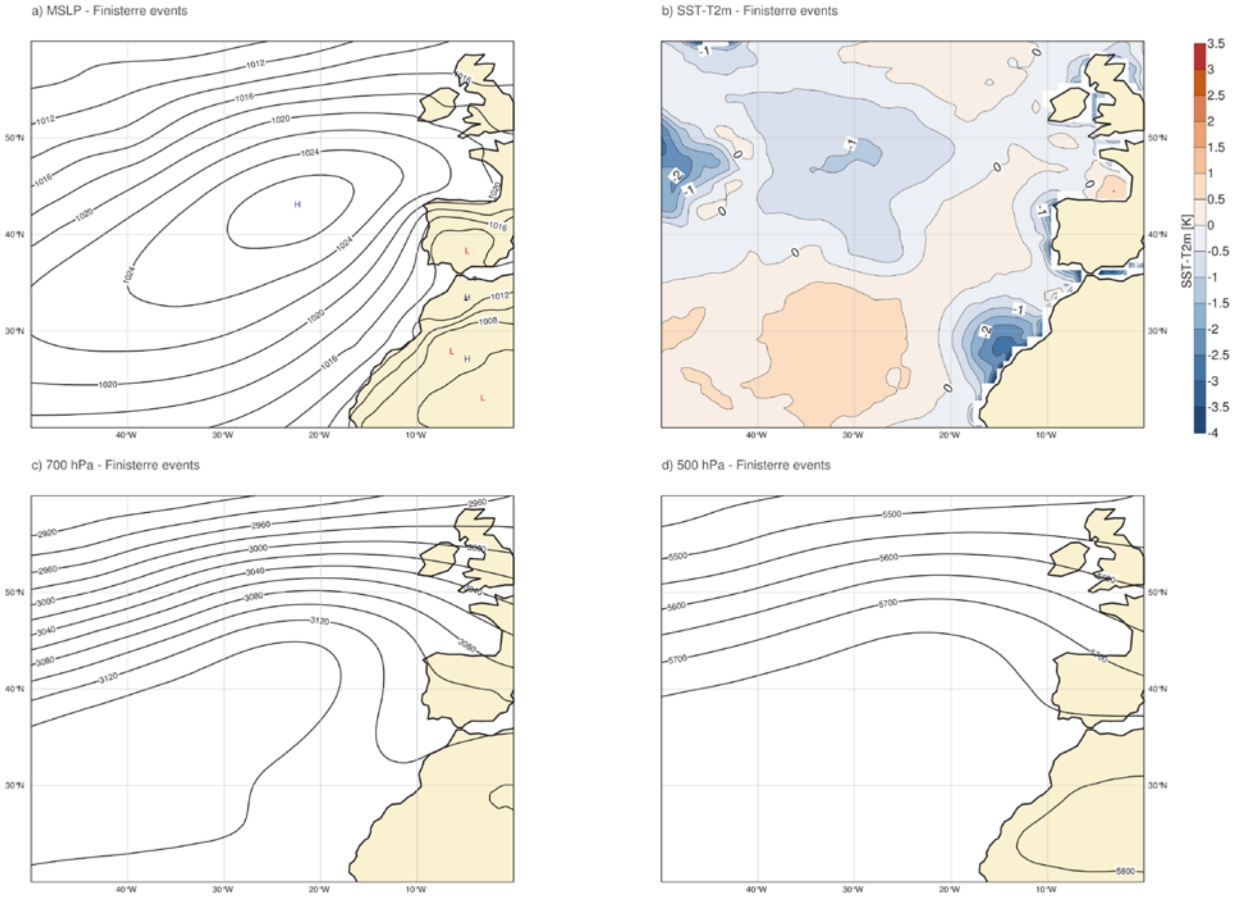

Figure 2. Average ERA-interim data for CJ conditions at Finisterre. Upper left: surface pressure; upper right: sea surface temperature; lower left: geopotential height at 700 hPa; lower right: geopotential height at 500 hPa.

As an example, figure 2 shows the average synoptic conditions as given by ERA-interim under coastal jet conditions at Finisterre. The high pressure area near the Azores is clearly visible. This system generates the southward flow along the Iberian coast necessary for the formation of coastal jets. The geopotential heights at 700 hPa and 500 hPa show that the Azores high is a surface phenomenon. Sea surface temperature shows upwelling of cold water along the Iberian coast and, even more prominent, along the North African west coast.

The synoptic conditions for occurrence of coastal jets at Roca and Finisterre show the same general picture as figure 2 (no results shown). Moreover, the results agree with those obtained from analyzing QuikSCAT data.

Buoy comparison

Table 2 gives the buoy comparison for all available ASCAT data during summer time in 2010 - 2014. The scatterometer wind products are labeled in the third column as A-6.25 for ASCAT-6.25 and as A-12.5 for ASCAT-coastal. Only collocations common to the two wind products are considered. The average (bias) and standard deviation (std. dev.) are shown for the difference in wind speed, zonal wind component *u* and meridional wind component *v*. The number of collocations is given by *N* in the last column.

The first pair of rows give the results for buoy collocations under all weather conditions. ASCAT-coastal compares slightly better to buoys in *u* and *v* than ASCAT-6.25, but slightly worse in wind speed. The differences, however, are small. The number of collocations is 1565, leading to an accuracy in the standard deviations of about 2.5%.

area	conditions	product	wind speed (m/s)		zonal *u* (m/s)		meridional *v* (m/s)		*N*
			bias	std. dev.	bias	std. dev.	bias	std. dev.	
All	all	A-6.25	0.146	1.00	0.039	1.71	0.093	1.60	1565
		A-12.5	0.177	1.02	0.033	1.68	0.087	1.56	
Finisterre	CJ	A-6.25	-0.14	0.82	-0.21	1.3	0.23	1.1	236
		A-12.5	-0.11	0.83	-0.25	1.3	0.18	1.1	
Roca	CJ	A-6.25	0.04	0.84	-0.04	1.7	0.13	1.5	223
		A-12.5	0.05	0.86	-0.07	1.7	0.19	1.5	
Vicente	CJ	A-6.25	0.03	0.89	0.09	1.5	0.07	1.4	409
		A-12.5	0.03	0.90	0.06	1.5	0.08	1.4	

Table 2 IPMA buoy comparison.

The next pairs of rows show results for Finisterre, Roca, and Vicente under CJ conditions. Now the number of collocations is much smaller, leading to accuracies of 5% to 7%. Nevertheless, the scatterometer winds compare better to buoy winds under CJ conditions, in particular for Finisterre.

The buoy winds were converted to 10 m neutral winds using the LKB model [*Liu et al.*, 1979]. This model depends on the Charnock coefficient, of which several values are recommended in the literature. In the data set studied here no significant dependency on the value of the Charnock coefficient was found (no results shown).

Table 3 shows the results for the global buoy comparison done by KNMI for August 2013 [*Vogelzang and Stoffelen*, 2016]. Only the standard deviations are shown in table 3. Comparison with the first pair of rows in table 2 (those for all areas under all conditions) shows that the standard deviations in wind speed are comparable, that those in the zonal wind component *u* are higher for the Iberian coast, and that those for the meridional wind component *v* are comparable for both the coastal product and ASCAT-6.25.

product	wind speed std. dev (m/s)	zonal wind std. dev. (m/s)	meridional wind std. dev. (m/s)	*N*
ASCAT-6.25	0.99	1.38	1.64	2682
ASCAT-coastal	0.98	1.36	1.59	2682

Table 3 KNMI global buoy comparison for August 2013.

The different behavior of *v* may be caused by representativeness problems. The buoy comparisons in tables 1 and 2 are based on buoy wind speeds and directions that were averaged over 10 minutes and issued every 10 minutes. As shown by *Lin et al.* [2015] it is better to compare scatterometer data with buoy winds averaged over a longer period, as a 10 minutes averaged buoy wind speed of 7 m/s is representative for a spatial scale of 4.2 km, whereas a scatterometer wind speed is representative for a much larger area (about 225 km^2 for ASCAT-6.25).

Triple collocation

Table 4 shows the error standard deviations conditions in *u* and *v* under CJ conditions for the buoys, for the two ASCAT wind products, and for the ECMWF background wind that comes with the ASCAT wind products. The precision in the final row is estimated under the assumption that the errors are Gaussian. The numbers in brackets refer to the Roca wind maxima events.

area	**product**	**buoys**		**ASCAT**		**ECMWF**		***N***
		σ_u (m/s)	**σ_v (m/s)**	**σ_u (m/s)**	**σ_v (m/s)**	**σ_u (m/s)**	**σ_v (m/s)**	
Finisterre	A-6.25	1.1	1.0	0.4	0.6	1.2	1.0	186
	A-12.5	1.2	1.0	0.4	0.6	1.1	0.9	173
Roca	A-6.25	1.5	1.3	0.5	0.9	0.8	1.2	170
	A-12.5	1.7	1.6	0.5	0.8	0.8	1.2	170
Vicente	A-6.25	1.0	0.9	0.6	0.6	1.1	1.3	302
	A-12.5	1.1	1.0	0.6	0.6	1.1	1.3	301
Precision		0.2 (0.4)	0.2 (0.4)	0.1	0.1	0.1	0.1	

Table 4. Triple collocation errors on the scatterometer scale(s).

Buoys in Roca maxima events seems to have larger errors than under Finisterre and Vicente events, though the errors in the error estimates are rather big due to the small number of collocations (see table 2). The errors in buoys, scatterometer wind products, and background found here are consistent with global values found in earlier studies. No significant difference between ASCAT-6.25 and ASCAT-coastal can be found from table 4. The last column in table 4 gives the number of collocations that were used for the final triple collocation analysis results.

Table 5 gives the calibration coefficients from the triple collocation analysis for the scatterometer and the background with respect to the buoys. The calibrated zonal wind component reads $u_{cal} = a_u u_{unc} + b_u$, with u_{cal} the linearly calibrated zonal wind and u_{unc} the uncalibrated one. A similar relation holds for the meridional wind component.

area	product	scatterometer				background			
		b_u (m/s)	b_v (m/s)	a_u	a_v	b_u (m/s)	b_v (m/s)	a_u	a_v
Finisterre	A-6.25	-0.07	-0.10	0.99	1.02	-0.06	0.54	0.96	1.10
	A-12.5	0.24	-0.23	0.98	0.99	0.92	-0.28	0.90	0.94
Roca	A-6.25	0.03	-0.10	0.92	0.97	0.34	0.35	0.85	0.99
	A-12.5	0.17	-0.12	0.89	0.93	0.48	0.40	0.85	0.98
Vicente	A-6.25	-0.07	-0.10	0.99	1.02	-0.06	0.54	0.96	1.10
	A-12.5	-0.00	-0.17	1.00	0.99	0.03	0.46	0.99	1.09

Table 5 Triple collocation calibration coefficients with respect to the buoys.

Table 5 shows that the scatterometer scalings a_u and a_v are close to one for Finisterre and Vicente, but not so for Roca. The scatterometer biases b_u and b_v may be quite large, notably for ASCAT-12.5. The background scalings differ considerably from one, and the biases may be over 0.54 m/s. This is an indication that the number of collocations is quite low, as already suggested by the numbers in table 4. As a result the errors are fairly large, so it is hard to draw firm conclusions from these tables.

Spatial statistics

In order to get more insight in the structure of the wind field, spatial variances were calculated for the 2° × 2° areas centered at the wind speed maxima for Finisterre, Roca, and Vicente. These areas are depicted in figure 1. Spatial variances are variances averaged over samples with varying size. They can be related to second-order structure functions [*Vogelzang et al.*, 2016]. Spatial variances are a direct measure of the cumulative variance as a function of scale.

Figure 3 shows the spatial variances of ASCAT-6.25 as a function of distance for the wind components *u* (left hand panels) and *v* (right hand panels) for the maximum wind areas at Finisterre (top panels), Roca (middle panels), and Vicente (bottom panels). Solid curves (labeled "average") give the spatial variance for the complete dataset. Dashed curves (labeled "CJ") give the results under coastal jet conditions, while dotted curves (labeled "non CJ") give the results under all other conditions. Only for Finisterre an extra category for wind reversal conditions (labeled "WR") is added. Blue curves pertain to along-track sampling, i.e.,sampling in the north-south direction while red curves are for cross-track (east-west) sampling.

On forehand one expects lower variability under CJ conditions than under non-CJ conditions. This is confirmed by figure 3, in all cases for scales less than about 100 km. At larger scales CJ variances may become larger than non-CJ variances in some cases, probably due to the finite size of the wind speed maximum. The largest variability is found under these wind reversal conditions at Finisterre. This is no surprise, as frontal passages mostly give rise to increased wind variability.

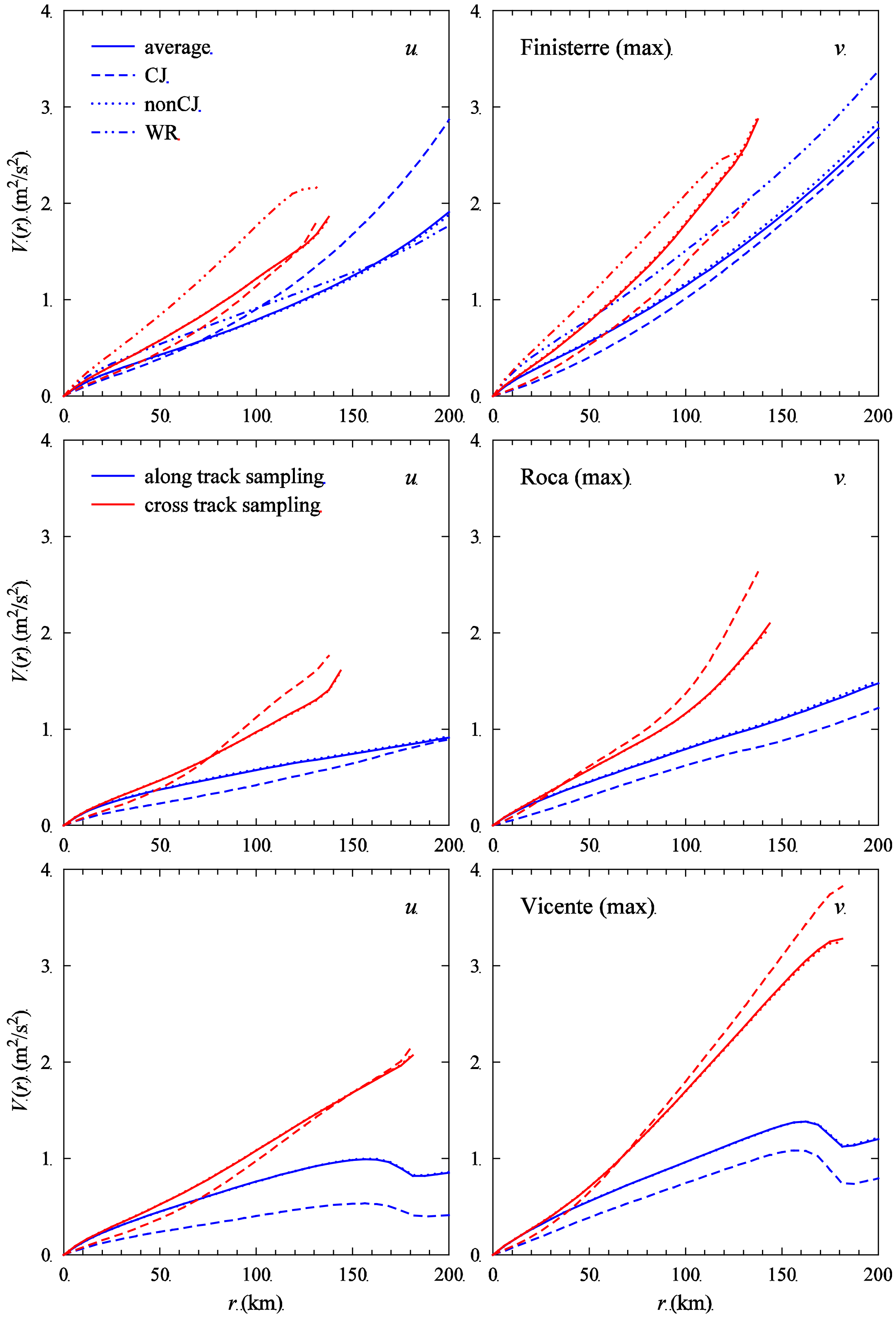

Figure 3. Spatial variances for the wind components *u* (left) and *v* (right) under various conditions.

Figure 3 also shows that cross-track sampling (red curves) yield higher variability than along-track sampling (blue curves), and that variability in *v* (right-hand panels) is mostly larger than that in *u* (left hand panels).

The first effect can be understood from figure 1 which shows that the wind direction more or less follows the capes. When sampling cross-track (in the east-west direction) this change in wind direction is included in each sample. When sampling along-track (north-south direction) the wind direction is more or less constant over a sample. The change in wind direction in cross-track samples will cause a trend in *u* and *v*. As the spatial variance is calculated with respect to the sample mean, this trend will increase the variance, hence the increased variability in cross-track sampling relative to along-track sampling.

The second effect, higher variability in *v* than in *u*, is less easy to explain. It does not show up in the IPMA buoy comparisons in table 2. Turbulent disturbances in the flow (with respect to the mean flow) are assumed isotropic, i.e., an obstruction would affect the 2D flow by generating shear vortices that generate similar-size amplitude disturbances in *u* and *v*. The energy is drawn from the mean flow, and cascaded in all directions generally. Maybe it has to do with organization in the turbulence due to boundary layer rolls of km size. These are organized perpendicular to the flow.

Note that the along-track results for Vicente show a maximum near a range of 160 km. This is most likely a sampling effect due to the fact that the northeastern part of the test area is land, causing systematically shorter along-track samples.

All ASCAT-6.25 spatial variances are higher than the corresponding ASCAT-coastal variances (no results shown), due to the larger noise in ASCAT-6.25.

User guidance

During processing of ASCAT-6.25 IPMA encountered some difficulties with the L1B full resolution data ordered from EUMETSAT. In order to reduce processing time, IPMA ordered only those parts of the data that covers the Iberian coast, using the selection tools on the EUMETSAT data ordering webpages. However, those files can not be read by AWDP, despite the fact that the data reading routines in AWDP precisely follow the EUMETSAT file format prescriptions for L1B full resolution data. This flaw in the data ordering has been brought to the attention of EUMETSAT, but is not yet fixed. The work-around is to use complete orbit files, not regional selections. This has been added to the AWDP user guide.

From March 2014 onwards one should use archived NRT files (ASCAT GDS Level 1 Sigma0 at Full Sensor Resolution - Metop). For earlier dates one should use reprocessed Climate Data Record files (ASCAT L1 SZF Climate Data Record Release 2 - Metop). One should not use archived NRT files earlier than March 2014, because these do not have the right format for high-resolution processing in AWDP. This has also been added in the AWDP user guide.

Since the operation of AWDP for generating ASCAT-coastal and ASCAT-6.25 wind products is quite complicated, an extra test folder has been added to the AWDP-v2.4 package containing L1B full resolution data, NWP grib files, and a Python script for organising the input data and running AWDP. The Python script contains extensive comments in order to enable users to adapt the script to their needs.

Discussion

Matters regarding user guidance have been treated with highest priority in order to have the AWDP-v2.4 release as complete as possible. As stated before, the experience at IPMA was most valuable for adding a separate high-resolution processing test folder in AWDP.

Scatterometers measure the small-scale sea surface roughness, which is related to the surface stress rather than the wind speed at 10 m anemometer height. The buoy comparisons and triple collocation analyses were done using buoy winds that were converted to 10 m neutral winds. It is better to include stability and pressure effects, and to convert the buoy winds to stress-equivalent winds.

Coastal jets occur under frequent summertime synoptic conditions, see figure 2. They occur in about 15% of the ASCAT overpasses at Finisterre and Roca, and in about 25% of the overpasses at Vicente. The more frequent occurrence at Vicente may be related to a delay between the maximum afternoon baroclinicity and the maximum evening winds. Better temporal scatterometer coverage would be helpful in this respect, because then more insight in the diurnal cycle may be obtained. Rapidscat data might be helpful in this respect.

Recommendations and further actions

IPMA and KNMI will continue their cooperation.

IPMA will convert the buoy winds to stress-equivalent winds including stability effects. IPMA will do the buoy comparison, KNMI the triple collocation analysis.

IPMA will collect all buoy data and calculate average buoy winds over longer time periods than 10 minutes in order to arrive at better representativeness for the scatterometer spatial scales.

IPMA will give their software for coastal jet detection to KNMI for application on RapidScat data to get more information on the diurnal cycle.

References

Lin, W., M. Portabella, A. Stoffelen, A. Verhoef, and A. Turiel, 2015.
ASCAT wind quality control near rain, *IEEE Trans. Geosci. Remote Sens.*, 53(8), 4165–4177.

Liu, W.T., K.B. Katsaros, and J.A. Businger, 1979,
Bulk parameterization of air-sea exchanges of heat and water vapor including the molecular constraints in the interface, *J. Atmos. Sci*., vol. 36.

Lourenço, A., I. T. Monteiro, S. Muacho and C. Barroso, 2015.
Operational use of ASCAT and JASON-2 data during the winter of 2013-2014 over the North East Atlantic. EUMETSAT Meteorological Satellite Conference Tolouse 2015.

Monteiro, I. T., 2015.
Validation of ASCAT Wind Products against Iberian Buoys during Coastal Jet Events. IPMA-DivMV Technical Report in preparation.

Monteiro, I. T., J. Vogelzang, and A. Stoffelen, 2015.
ASCAT-6.25 validation on coastal jets. NWPSAF report NWPSAF-KN-VS-015.

Stoffelen, Ad, Wenming Lin and Marcos Portabella, 2013.
ASCAT scatterometer wind variability, in Pilot course on the use of satellite winds and wave data for marine safety forecasting in African waters, by EUMETSAT, NOAA, SAWS, KNMI, http://training.eumetsat.int/pluginfile.php/10440/mod_folder/content/0/ASCAT_MLE.ppt?forcedownload=1.

Vogelzang. J., G.P. King, and A. Stoffelen, 2015.
Spatial variances of wind fields and their relation to second-order structure functions and spectra, *J. Geophys. Res. Oceans*, 120, doi:10.1002/2014JC010239.

Verhoef, A., J. Vogelzang, J. Verspeek, and A. Stoffelen, 2016.
AWDP User manual and Reference Guide, version 2.4. NWP SAF report NWPSAF-KN-UD-005.

Vogelzang, J., and A. Stoffelen, 2016.
ASCAT-6.25 validation, NWP SAF Technical Report NWPSAF-KN-TV-009.